Electronic Supplementary Information (ESI)

Incorporation of organic crystals in the interspace of oriented nanocrystals: morphologies and properties

Yurika Munekawa, Yuya Oaki,* Kosuke Sato, Hiroaki Imai*

Department of Applied Chemistry, Faculty of Science and Technology, Keio University, 3-14-1 Hiyoshi, Kohoku-ku, Yokohama 223-8522, Japan

E-mail: oakiyuya@applc.keio.ac.jp, hiroaki@applc.keio.ac.jp

Contents

Experimental section

Introduction of the Organic Crystals in the Oriented Nanocrystals. The sea urchin spines of *Echinometra mathaei* were used as a model of the oriented nanocrystals. The biomineral was immersed in 5 wt.-% sodium hypochlorate (NaClO) aqueous solution for 24 h to remove the incorporated biological macromolecules. The same treatment was performed in the fresh NaClO aqueous solution, again. After the washing by purified water, the sea urchin spines were treated at 450°C for 4 h in air to expand the nanospace for the incorporation of the monomer. The organic crystals, such as VCz (TCI, 98 %), AB (Kanto), and PY (Kanto), were used without purification. An excess amount of organic crystals, typically 5–10 mg, and a sea urchin spine were placed on a glass slide. The glass slide was maintained on a heating stage at 75 ˚C for VCz, 90 ˚C for AB, and 180 ˚C for PY to obtain the melts. After 10–20 min., the sea urchin spine was withdrawn from the melts. The excess amount of the melt was immediately absorbed by a paper towel before the cooling. The sample with the macroscopic shape of a sea urchin spine was put in a purified water, typically 20 cm^3, with the treatment in an ultrasonic bath for about 10 min. The organic crystals remaining in the micrometer-scale pores of the sponge morphology were physically removed by the treatment in the ultrasonic bath. After the decantation, the sample was washed by purified water several times and then dried at room temperature. In this way, the composites of the original materials and the incorporated organic crystals were obtained. For the morphology replication, the original $CaCO_3$ material was dissolved by hydrochloric acid (HCl). The composite with the morphology of a sea urchin spine was put in 5 cm^3 of 0.1 mol dm^{-3} HCl solution for 24 h. After washing by purified water, the sample was dried at room temperature under ambient pressure. The hierarchically replicated materials were obtained in this procedure. The exoskeleton of a sea star (*Linckia laevigata*) was used as another original material. The vaterite spheres consisting of the oriented nanocrystals were synthesized by the methods reported in our previous work.[15] As for these samples, the VCz crystals were introduced by the same procedure including the pretreatments.

Morphology Observation: Morphologies of the resultant materials were observed by SEM (Keyence VE-9800) and FESEM (Hitachi S4700 and FEI Sirion) operated at 5.0 kV. The samples were coated by an ultrathin amorphous osmium (Vacuum Device, HPC-1S) for 10 sec. The nanostructures were observed by FETEM (FEI Tecnai F20) operated at 200 kV. The dispersion liquids of the powdered samples were prepared in purified water or ethanol and then dropped on a collodion membrane supported by copper grid.

Contents of the Organic Crystals: The contents of the organic crystals incorporated in the original materials were analyzed by the TG (Seiko TG/DTA 6200 and TG/DTA 7200).

Crystallinity: The crystallinity was measured by XRD. The wide and narrow $2\theta/\theta$ scans, as shown in Fig. 4a,b, were performed by Rigaku MiniFlex II and Bruker AXS D8-Advance, respectively. The size of the crystallites (t) was estimated from the Scherrer's equation by the following procedure (eq. S1):

$t = K\lambda/B\cos\theta$ … (eq. S1)

where K is the constant (K=0.9), λ is the wavelength of Cu-Kα line (λ=0.154 nm), B is the half maximum full-width of the peak, and θ is the diffraction angle of the peak. Powder of a commercial single crystal of $CaCO_3$ ca. 1 µm in size (Kanto, 99.5%) was used as the reference for the correction of B. The B of the (104) plane of the reference sample was subtracted from the observed B of the samples. The SAED and HRTEM observations were performed by using FETEM.

Thermal Properties: The T_m and T_f of the organic crystals were analyzed by DSC (Rigaku, Themo plus2). The powdered samples, ca. 10 mg, were put in the sample pan. The heating and cooling rates were 10 K min^{-1} at the first cycle and 2 K min^{-1} at the second and third cycles.

Photochemical Properties: The UV-Vis absorption spectra of AB were measured on the powdered samples by using JASCO V-670 equipped with an integrating sphere. The photoluminescent spectra of PY were measured on the powdered samples by using JASCO FP-6500.

Polymerization: The polymerization of the VCz was performed on the composite of the $CaCO_3$ original material and VCz. The composite with the morphology of a sea urchin spine was immersed in 1 cm^3 of the chloroform solution containing 0.1 mol dm^{-3} $FeCl_3$ under –18 °C. After 1 h, 10 cm^3 of methanol was added in the sample vessel to stop the polymerization reaction. Then, the resultant sample was washed by methanol several times. The composite was put in 5 cm^3 of 0.1 mol dm^{-3} HCl solution for 24 h. After washing by purified water, the sample was dried at room temperature under ambient pressure. The hierarchically replicated materials were obtained in this procedure. The polymerized objects were characterized by KBr method of FT-IR (Bruker, Alpha-T). A commercial PVCz powder (TCI) was used as the reference without purification.

Formation of CT complex: The toluene solution, typically 0.5 cm^3, containing 400 mmol dm^{-3} TNF was prepared at 100 °C by using a heating stage. The commercial PVCz powder and the resultant hierarchical PVCz, each 39.4 mg, were immersed in the TNF toluene solution for 10 sec. After stopping of the heating, 5 cm^3 of acetone was added to the sample vessel. The sample was withdrawn and then washed with 50 cm^3 of acetone to remove the excess TNF. The amount of the CT complex with TNF was estimated from the FT-IR spectra. The detailed methods were described with Fig. S7 in the Supporting Information.

TG curves of the composites

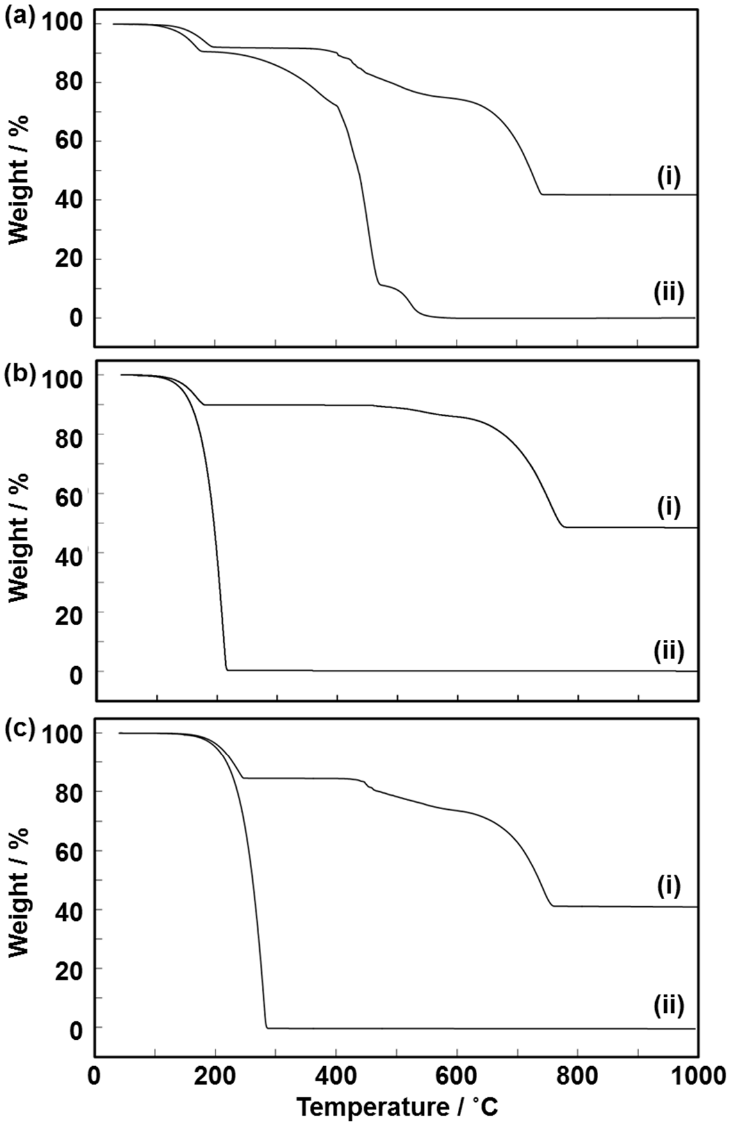

Fig. S1. TG curves of the composites based on VCz (a), AB (b), and PY (c). The spectra (i) and (ii) correspond to the composites and the commercial organic crystals respectively.

The biological macromolecules remained in the sample of sea urchin spines. The weight of the remaining biological macromolecules was subtracted. The weights had the individual differences on the samples. The contents of the incorporated organic crystals were estimated to be 15.2 wt.% for VCz, 10.4 wt.% for AB, and 15.4 wt.% for PY.

FESEM images of the AB and PY replicated architectures

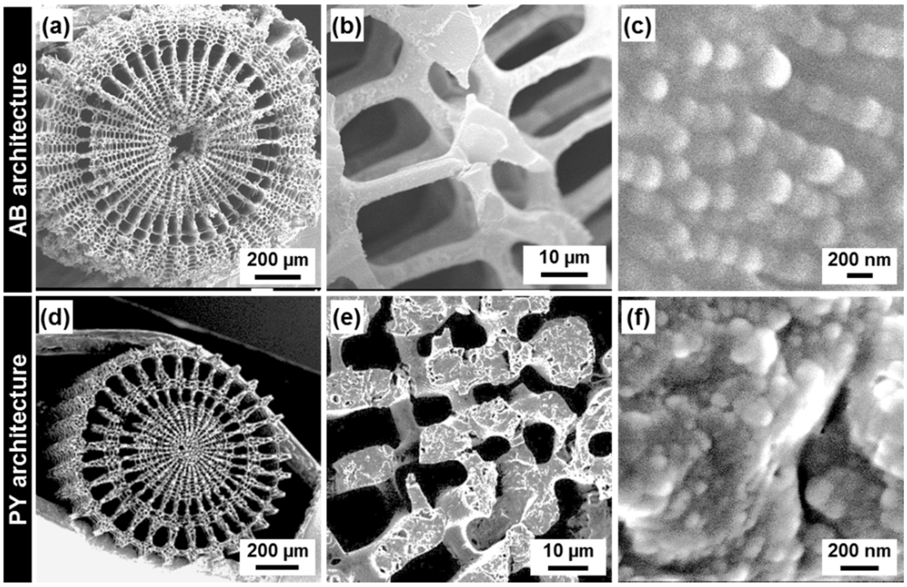

Fig. S2. FESEM images of the replicated architectures of AB (a–c) and PY (d–f) crystals.

The hierarchical morphologies of the original material were replicated to AB and PY crystals. In micrometer scale (Fig. S2b,e), the inside parts of the sponge skeletal body were not completely replicated to the organic crystals. The surface parts of the sponge skeletal body were only replicated to the organic crystals because of the viscosity of the melts. The reasons were discussed in the main text.

The hierarchical VCz architectures replicated from the other original materials

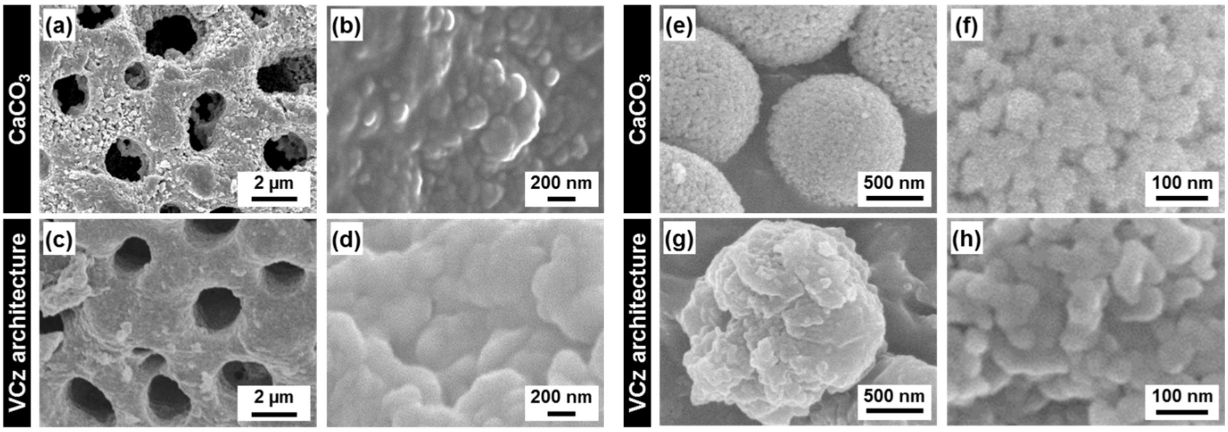

Fig. S3. Hierarchical morphology replication from the other original materials (a,b,e,f,) to the VCz architectures (c,d,g,h). (a–d) FESEM images of the exoskeleton of a sea star (a,b) and its replicated VCz architecture (c,d). (e–h) the synthetic vaterite oriented nanocrystals with the spherical morphology (e,f) and the replicated VCz architecture (g,h).

The similar hierarchical morphology replication was achieved on the other original materials, such as the exoskeleton of a sea star and the synthetic oriented nanocrystals of vaterite $CaCO_3$. The method for preparation of the vaterite spheres was referred to our previous report.[15] The results suggest that the approach can be applied to a variety of original materials with the hierarchical structures.

XRD patterns of the AB and PY samples

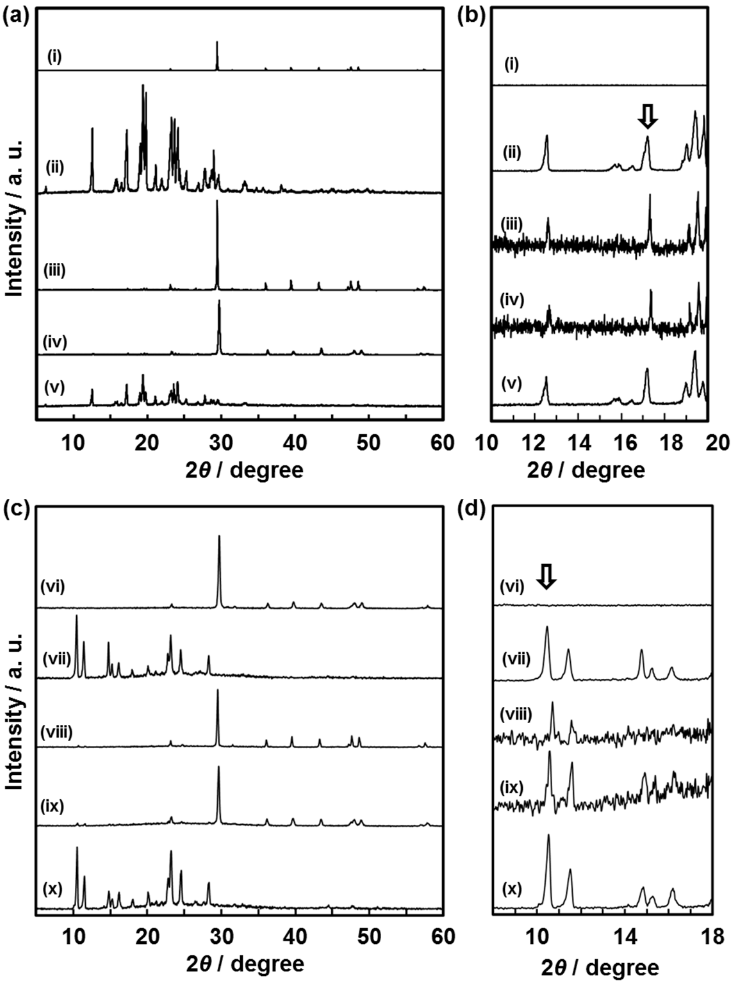

Fig. S4. XRD patterns (a,c) and their magnified ones (b,d) to study the crystallinity of the AB (a,b) and PY (c,d) with incorporation in the oriented nanocrystals. The profiles (i)–(x) represent the following samples: (i, vi) the exoskeleton of a sea urchin spine before the incorporation of the AB and PY respectively, (ii, vii) the commercial organic crystals, (iii, viii) the commercial samples recrystallized with a commercial $CaCO_3$ powder, (iv, ix) the composite after the incorporation of the organic crystals in the exoskeleton of a sea urchin spine, (v, x) the replicated architectures after the dissolution of the original calcite.

The *B* and *t* were estimated from the peaks marked by the white arrows in the panels (b,d) (Table 1 in the main text). The samples (iii) and (iv) contained the same amount of AB. The samples (viii) and (ix) contained the same amount of PY.

Photochemical properties of the incorporated AB and PY

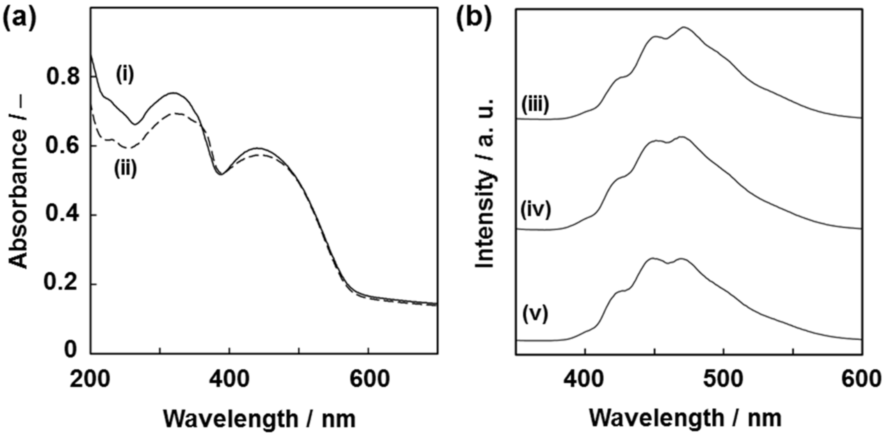

Fig. S5. Photochemical properties of the incorporated AB (a) and PY (b) in the interspace of the oriented nanocrystals. (a) UV-Vis absorption spectra of AB before (i) and after (ii) the irradiation of UV light at 365 nm. (b) photoluminescence spectra of commercial PY crystal (iii), the PY incorporated in the oriented nanocrystals (iv), and the replicated PY architecture (v) with UV light excitation at 330 nm.

These results indicate that the incorporated organic crystals showed the same photochemical properties as those of the bulk state. The XRD and SAED patterns also support the formation of the single-crystalline structures in the interspace of the oriented nanocrystals.

DSC thermograms of the AB and PY samples

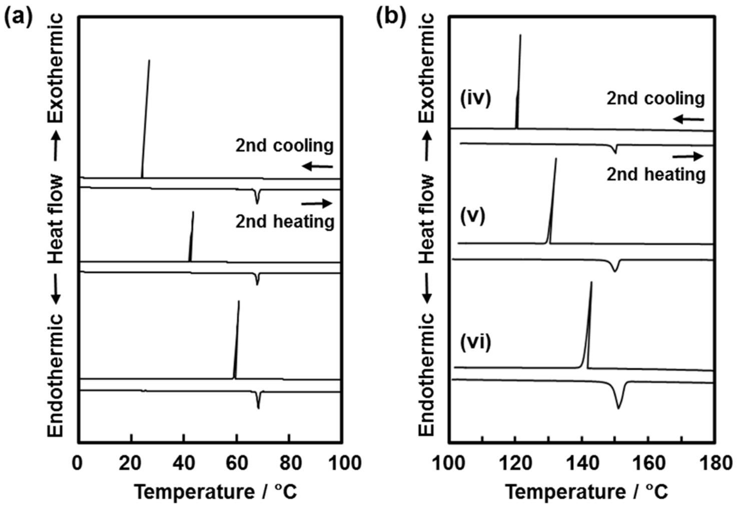

Fig. S6. DSC thermograms of AB (a) and PY (b) samples. The thermograms (i)–(vi) correspond to the following samples: (i, iv) commercial powders of AB and PY respectively, (ii, v) the mixture of a commercial calcite with the commercial AB and PY crystals respectively, (iii, vi) the mixture of a sea urchin spine and commercial AB and PY crystals respectively. All the data were obtained from the second heating and cooling processes. The onset temperature was used for the estimation of T_m and T. in Table 2.

The data of T_m and T_f were summarized in Table 2 in the main text. In all the cases, only the T_f was raised on the organic crystals with incorporation in the interspace of the oriented nanocrystals, while T_m was not changed.

FT-IR spectra for the formation of CT complex between PVCz and TNF

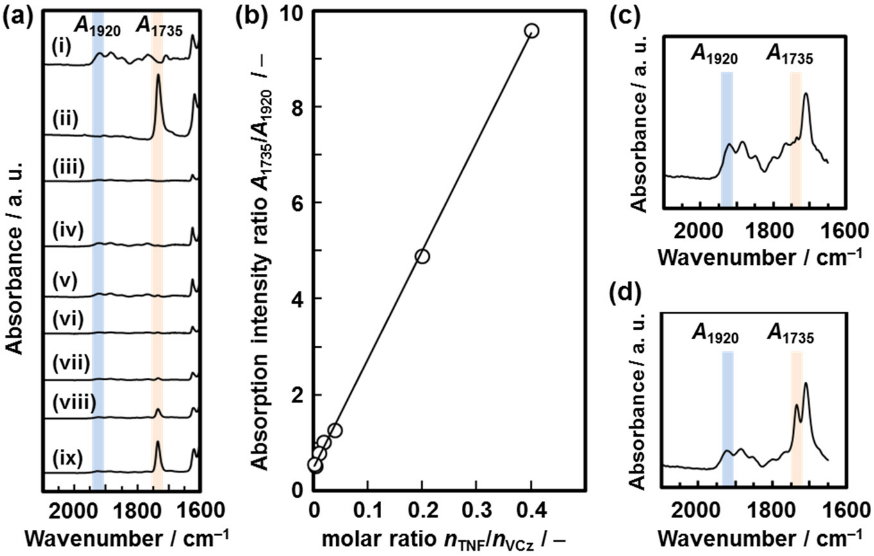

Fig. S7. Estimation of the amount of CT complex formation between PVCz and TNF. (a) FT-IR spectra of the resultant CT complex formed by variation of molar ratio of TNF (n_{TNF} / mol) to the VCz monomer units in the PVCz molecule (n_{VCz} / mol) ($R=n_{\mathrm{TNF}}/n_{\mathrm{VCz}}$). The spectra (i)–(ix) correspond to the following samples: (i) the commercial PVCz crystal (R=0), (ii) the commercial TNF, (iii) R=0.002, (iv) R=0.004, (v) R=0.01, (vi) R=0.02, (vii) R=0.04, (viii) R=0.2, (ix) R=0.4. (b) the relationship between the R (horizontal axis) and the absorption intensity ratio (A_{1735}/A_{1920}) (vertical axis) at 1735 cm^{-1} (A_{1735}) and 1920 cm^{-1} (A_{1920}) assigned to TNF and VCz unit, respectively. (c,d) FT-IR specra of the CT complex based on the commercial PVCz powder (c) and the resultant hierarchical PVCz architecture (d).

The calibration curve in the panel (b) was prepared by the data in the panel (a). The formation of the CT complex in the standard samples was performed in the tetrahydrofuran (THF) solution of the PVCz and TNF mixed by the specified molar ratio ($R=n_{\mathrm{TNF}}/n_{\mathrm{VCz}}$=0.002~0.4). All the dissolved TNF is regarded as the formation of the CT complex with an excess amount of PVCz in the solution phase. After the evaporation of THF, the FT-IR spectra of the precipitates were obtained (Fig. S7a). The peak intensity ratio of A_{1735}/A_{1930} is proportional to the TNF content in the PVCz, namely R. Therefore, the calibration curve was prepared as shown in Fig. S7b. Based on the spectra in Fig. S7c,d, the amount of the CT complex was calculated on the samples prepared from the commercial PVCz powder and the resultant hierarchical PVCz.